

The α -Law of Observable Belief Revision in Large Language Model Inference

Mike Farmer*

Abhinav Kochar[†]Yugyung Lee[‡]

Abstract

Large language models (LLMs) that iteratively revise their outputs—via chain-of-thought, self-reflection, or multi-agent debate—lack principled guarantees on the stability of their probability updates. We identify a consistent multiplicative scaling law governing how instruction-tuned LLMs revise probability assignments over candidate answers: $\log q_1(i) = \alpha[\log q_0(i) + \log b(i)] + c$, where α is a *belief revision exponent* and b is evidence from verification. We prove that $\alpha < 1$ is necessary and sufficient for asymptotic stability under iterated revision. Empirical validation across 4,975 problems, four graduate-level benchmarks (GPQA Diamond, TheoremQA, MMLU-Pro, ARC-Challenge), and two primary model families (GPT-5.2, Claude Sonnet 4) yields $\alpha = 1.163 \pm 0.084$ with mean $R^2 = 0.76$ —models exhibit near-Bayesian update behavior, slightly above the stability boundary. While single-step α exceeds 1, multi-step validation on 198 GPQA problems over 7 revision steps shows α decays from 0.84 to 0.54, yielding contractive long-run dynamics consistent with the stability theorem. Token-level logprob validation on 191 problems with Llama-3.3-70B confirms median $\alpha \approx 1.0$ for both logprob and self-reported elicitation. Decomposing the update into prior and evidence components reveals architecture-specific *trust*

ratio fingerprints: GPT-5.2 exhibits balanced weighting ($\tau \approx 1.0$) while Claude shows slight evidence-favoring ($\tau \approx 1.1$). This work characterizes observable inference-time update behavior; it does not claim that LLMs internally perform Bayesian inference. The α -law provides a principled diagnostic for monitoring observable update quality in LLM inference systems.

1 Introduction

Iterative refinement is widely used in language model inference—chain-of-thought prompting, self-reflection, multi-agent debate, and tree-of-thought search all involve repeated revision of probability assignments. Yet the mathematical structure of these updates remains poorly understood. *When a model revises its output probabilities in light of new evidence, is the resulting update stable?*

This question has practical consequences. If the geometry of iterative updates is *expansive* rather than *contractive*, errors compound rather than correct. Huang et al. (2024) showed that LLMs cannot reliably self-correct reasoning without external feedback, highlighting the need for principled analysis of update dynamics.

We approach this problem through the lens of control theory: rather than treating belief revision as a black box, we characterize its mathematical structure. Our central finding is that instruction-tuned LLMs exhibit a remarkably simple and consistent update rule in their observable output probabilities.

Scope. This work characterizes observable inference-time update behavior. We measure

*Bloch School of Management, Regnier Institute for Entrepreneurship & Innovation, University of Missouri–Kansas City. farmerm@umkc.edu

[†]Department of Computer Science, School of Science and Engineering, University of Missouri–Kansas City. arkrnr@umkc.edu

[‡]Department of Computer Science, School of Science and Engineering, University of Missouri–Kansas City. leeyu@umkc.edu

how model-reported probability distributions change when evidence is presented. We do not claim that LLMs internally perform Bayesian inference or that the measured exponent reflects a specific training-level mechanism.

Theory–empirics bridge. The theoretical stability condition (Theorem 1) requires $\alpha < 1$ for contractive dynamics. Our single-step empirical measurements yield $\alpha \approx 1.16 > 1$, indicating mildly expansive individual updates. This apparent tension is resolved by multi-step experiments showing that α decreases systematically under iteration (from 0.84 to 0.54 over 7 steps), yielding contractive long-run dynamics with geometric mean $\bar{\alpha}_{\text{geo}} = 0.75 < 1$. The theorem thus identifies the stability boundary that empirical trajectories must eventually cross, and our data show that they do.

Contributions. We make three contributions:

1. **The α -law** (Section 3). We identify a consistent multiplicative scaling law governing belief revision in instruction-tuned LLMs: $\log q_1(i) = \alpha[\log q_0(i) + \log b(i)] + c$. We prove that $\alpha < 1$ is necessary and sufficient for contraction in KL divergence, establishing a theoretical foundation for belief stability analysis. Empirically, we find $\alpha = 1.163 \pm 0.084$ —near-Bayesian updating with slight overconfidence.
2. **Comprehensive validation** (Sections 5–6). We validate the α -law across 4,975 problems on four graduate-level benchmarks with two primary model families. We further validate via multi-step revision (198 problems, 7 steps), token-level logprob comparison (191 problems), K -ablation, and identifiability analysis.
3. **Trust ratio fingerprints** (Section 5). Decomposing α into prior and evidence components reveals that model families exhibit distinct evidence-weighting strategies, with implications for robustness and controllability.

2 Background and Related Work

Self-correction in LLMs. Recent work has explored various mechanisms for LLM self-correction, including chain-of-thought prompting (Wei et al., 2022), self-refinement (Madaan et al., 2023), verbal reinforcement learning (Shinn et al., 2023), and multi-agent debate (Du et al., 2023; Liang et al., 2023). These approaches improve performance empirically but lack theoretical guarantees on convergence or stability. Self-consistency methods (Wang et al., 2023) aggregate multiple samples but do not characterize the geometry of individual belief updates.

Confidence calibration. Work on LLM calibration (Kadavath et al., 2022; Lin et al., 2022) has established that model-reported probabilities are often poorly calibrated. Temperature scaling (Guo et al., 2017) adjusts output distribution sharpness uniformly but does not address the geometry of iterative updates. Our α -law characterizes something distinct: the multiplicative structure of how models integrate prior beliefs with new evidence.

Generalized Bayesian updating and tempered inference. The α -law is formally equivalent to the tempered (or power) posterior of Grünwald & van Ommen (2017) and Holmes & Walker (2017) with tempering parameter $\eta = \alpha$. The broader framework of generalized Bayesian updating (Bissiri et al., 2016) replaces the log-likelihood with an arbitrary loss function, yielding posteriors of the form $\pi(\theta|x) \propto \pi(\theta) \exp(-\eta \ell(\theta, x))$, where η controls the learning rate. Grünwald (2012) introduced SafeBayes, which adaptively selects η to ensure consistency under model misspecification. In calibration, Gneiting & Raftery (2007) established the theory of proper scoring rules that underlies principled probability evaluation.

The contribution here is not the functional form but the empirical finding that large language models spontaneously exhibit tempered Bayesian revision when prompted to update probabilities, with

α constrained to a narrow, model-specific range. Where prior work treats the tempering parameter as a tunable hyperparameter chosen *prescriptively* for robustness, we show that α emerges as a measurable *property* of each model family’s observable output behavior—one that distinguishes vendor architectures and degrades predictably under noise. The α -law thus reframes tempered posteriors from a prescriptive tool to a descriptive lens for LLM inference behavior. Xie et al. (2022) provide complementary theoretical grounding by showing that in-context learning can be understood as implicit Bayesian inference, suggesting a mechanism by which such structure could arise.

Test-time compute scaling. Snell et al. (2024) demonstrate that adaptively scaling inference-time computation can outperform parameter scaling. Their framework optimizes *how much* compute to allocate but treats the belief update mechanism as fixed. Verification approaches (Lightman et al., 2023; Cobbe et al., 2021) provide evidence signals but do not characterize how models integrate this evidence. Our work complements these by characterizing the *geometry* of belief revision itself.

3 The α -Law of Belief Revision

3.1 Setup and Notation

Consider a system maintaining a belief distribution $q_t \in \Delta^{K-1}$ over K candidate answers. At each revision step, the system receives evidence $b_t \in \Delta^{K-1}$ from verification and produces updated belief q_{t+1} .

Standard Bayesian updating prescribes:

$$q_{t+1}(i) \propto q_t(i) \cdot b_t(i) \quad (1)$$

which in log-space becomes $\log q_{t+1}(i) = \log q_t(i) + \log b_t(i) + c_t$ with slope 1 on both terms.

3.2 The Multiplicative Update Law

We propose and empirically validate that LLM belief revision follows:

$$\boxed{\log q_{t+1}(i) = \alpha[\log q_t(i) + \log b_t(i)] + c_t} \quad (2)$$

where $\alpha > 0$ is the *belief revision exponent* and c_t ensures normalization. Equivalently, $q_{t+1} \propto (q_t \cdot b_t)^\alpha$.

Note: Equation (2) describes the observable relationship between model-reported probability distributions before and after evidence presentation. It does not imply that the model internally computes a Bayesian update or that α corresponds to an explicit parameter in the model’s architecture.

This update arises as the stationary condition of a KL-regularized variational objective:

$$J[q] = \alpha D_{\text{KL}}(q||q_t) - \mathbb{E}_q[\log b_t] \quad (3)$$

where $\alpha = 1/(1 + \lambda)$ and $\lambda \geq 0$ is regularization strength.

3.3 Stability Analysis

Theorem 1 (α -stability). *Let q^* be a fixed point of update (2) for fixed evidence b . If $\alpha < 1$, then q^* is asymptotically stable:*

$$D_{\text{KL}}(q_t||q^*) \leq \alpha^{2t} D_{\text{KL}}(q_0||q^*) \quad (4)$$

If $\alpha \geq 1$, the fixed point is unstable under perturbation.

This yields three regimes with distinct dynamical properties:

Table 1: Three regimes of belief revision dynamics determined by the α exponent.

Regime	Cond.	Behavior
Contractive	$\alpha < 1$	Stable. Errors decrease geometrically at rate α^{2t} .
Bayesian	$\alpha = 1$	Marginal stability. Full commitment to likelihood ratio.
Expansive	$\alpha > 1$	Unstable. Errors amplify exponentially each step.

Extension to time-varying α . Theorem 1 assumes a fixed α across steps. When α varies per step (as observed empirically in Section 6.1), the contraction bound generalizes to:

$$D_{\text{KL}}(q_T||q^*) \leq \left(\prod_{t=0}^{T-1} \alpha_t^2 \right) D_{\text{KL}}(q_0||q^*) \quad (5)$$

Convergence is thus guaranteed whenever $\prod_t \alpha_t^2 \rightarrow 0$, i.e., when the geometric mean of α_t is less than 1. Our multi-step data (Section 6.1) yields $\bar{\alpha}_{\text{geo}} = (\prod_{t=1}^7 \alpha_t)^{1/7} = 0.75$, well within the contractive regime. This bridges the apparent tension between the single-step finding ($\alpha \approx 1.16 > 1$) and the stability requirement ($\alpha < 1$): although individual updates are mildly expansive, the systematic decay of α under iteration drives the cumulative product below the stability boundary.

3.4 Extended Two-Parameter Model

Relaxing the constraint that prior and evidence receive equal weight:

$$\log q_{t+1}(i) = \alpha_{q_0} \log q_t(i) + \alpha_b \log b_t(i) + c_t \quad (6)$$

The *trust ratio* $\tau \equiv \alpha_b / \alpha_{q_0}$ quantifies evidence trust relative to prior:

- $\tau > 1$: Evidence-amplifying (responsive but vulnerable)
- $\tau < 1$: Prior-anchoring (robust but resistant to correction)
- $\tau = 1$: Balanced weighting (Bayesian-like)

3.5 Empirical Interpretation: Near-Bayesian α

Our empirical finding of $\alpha \approx 1.16$ places instruction-tuned LLMs in the *near-Bayesian* regime—slightly above the stability boundary established by Theorem 1—under the evidence encoding described in Section 4.3. This is a positive finding: LLMs closely approximate optimal rational inference, with only $\sim 16\%$ more aggressive updating than perfect Bayes.

Bridging theory and empirics. Theorem 1 establishes that $\alpha < 1$ is necessary and sufficient for stability when α is *fixed* across iterations. Our empirical single-step finding of $\alpha > 1$ therefore indicates that a single revision step is mildly expansive. However, the multi-step validation (Section 6.1) reveals that α is not fixed: it decreases systematically

with revision depth, from $\alpha_1 = 0.84$ to $\alpha_7 = 0.54$. For time-varying α_t , the relevant stability condition is that the product $\prod_{t=1}^T \alpha_t < 1$, which is satisfied whenever the geometric mean $\bar{\alpha}_{\text{geo}} = (\prod \alpha_t)^{1/T} < 1$. In our data, $\bar{\alpha}_{\text{geo}} = 0.74$ over 7 steps, well within the contractive regime. The theorem thus provides the correct reference frame: it identifies the stability boundary that empirical α trajectories must eventually cross, and our data show that they do.

4 Experimental Setup

4.1 Datasets

We evaluate across four graduate-level benchmarks spanning diverse reasoning domains:

- **GPQA Diamond** (Rein et al., 2023): 198 graduate-level science questions (physics, chemistry, biology)
- **TheoremQA** (Chen et al., 2023): 800 theorem-application problems in mathematics
- **MMLU-Pro** (Wang et al., 2024): 490 multi-subject reasoning problems with 10 answer options
- **ARC-Challenge** (Clark et al., 2018): 700 commonsense reasoning questions

4.2 Models

We evaluate three categories of models:

- **Primary (single-step):** GPT-5.2 (OpenAI, 2024) and Claude Sonnet 4 (Anthropic, 2024)—state-of-the-art instruction-tuned models with high data quality ($>95\%$ clean rate)
- **Multi-step validation:** GPT-4 for iterated revision experiments with simulated verifier feedback (Section 6.1)
- **Logprob validation:** Llama-3.3-70B-Instruct (Grattafiori et al., 2024) via Together.ai for token-level logprob access (Section 6.2)

Gemini 2.5 Flash was tested but excluded from primary analysis due to a 68.7% fallback contamination rate (Section 5.4).

4.3 Protocol

For each problem instance, we execute a four-step protocol:

1. **Generate:** Produce $M = 8$ candidate solutions via nucleus sampling ($T = 0.7$)
2. **Elicit prior:** Obtain pre-reflection beliefs $q_0(i)$ via structured probability elicitation
3. **Verify:** Check candidates using deterministic verification (numerical comparison, unit tests)
4. **Elicit posterior:** Obtain post-reflection beliefs $q_1(i)$ after presenting verification results

The evidence distribution $b(i)$ is constructed from verification outcomes. For multiple-choice benchmarks (GPQA, MMLU-Pro, ARC-Challenge), we assign $b(i) = 0.9$ to the verified correct answer and $b(j) = (0.1)/(K - 1)$ to each incorrect option, reflecting a strong but imperfect verifier signal. For theorem-application problems (TheoremQA), the same scheme applies after matching candidate solutions to the ground truth. This asymmetric evidence structure ensures that the predictor $\log q_0(i) + \log b(i)$ spans a wide range, enabling reliable OLS estimation of α . Full details of evidence computation are in Appendix B.

The α -law regression then computes $x_i = \log q_0(i) + \log b(i)$ and $y_i = \log q_1(i)$, fitting $y_i = \alpha x_i + c$ via ordinary least squares (OLS).

4.4 Data Quality Filtering

To ensure α -law measurements reflect genuine LLM belief revision rather than fallback heuristics, we apply strict data quality filtering:

- Include only records where the posterior q_1 was directly elicited from the LLM (source method = “llm”)

- Exclude models with $>20\%$ fallback contamination rate
- Require valid probability distributions (all entries positive, sum to 1)

Scope of generalization. Results are validated on instruction-tuned language models accessed via commercial APIs. The α -law may not generalize to base (non-instruction-tuned) models, non-elicited belief representations, or modalities beyond text.

5 Results

5.1 Core α -Law Validation

Figure 1 visualizes the α -law across model \times dataset combinations. Each point represents a single problem; the clustering around the regression line confirms the multiplicative structure of belief revision.

Table 2 presents the complete results. On clean (LLM-only) data, all model \times dataset combinations yield $\alpha \approx 1.0$ – 1.3 with R^2 ranging from 0.59 to 0.90 (mean $R^2 = 0.76$), indicating consistent near-Bayesian belief revision.

Observation 1: Near-Bayesian α . The mean $\alpha = 1.163 \pm 0.084$ across all clean model \times dataset combinations indicates that instruction-tuned LLMs perform near-Bayesian belief revision under our verification protocol (Section 4.3). This slight overconfidence ($\sim 16\%$ above Bayesian optimal) is consistent across both model families and all four benchmarks. We note that α is measured relative to the specific evidence encoding $b(i)$; different evidence constructions would yield different absolute α values (see Section 8).

5.2 Cross-Model Consistency

Observation 2: Architecture independence. As shown in Figure 2(a), both model families exhibit statistically indistinguishable α distributions, suggesting the α -law reflects a general property of instruction-tuned LLMs rather than a model-specific

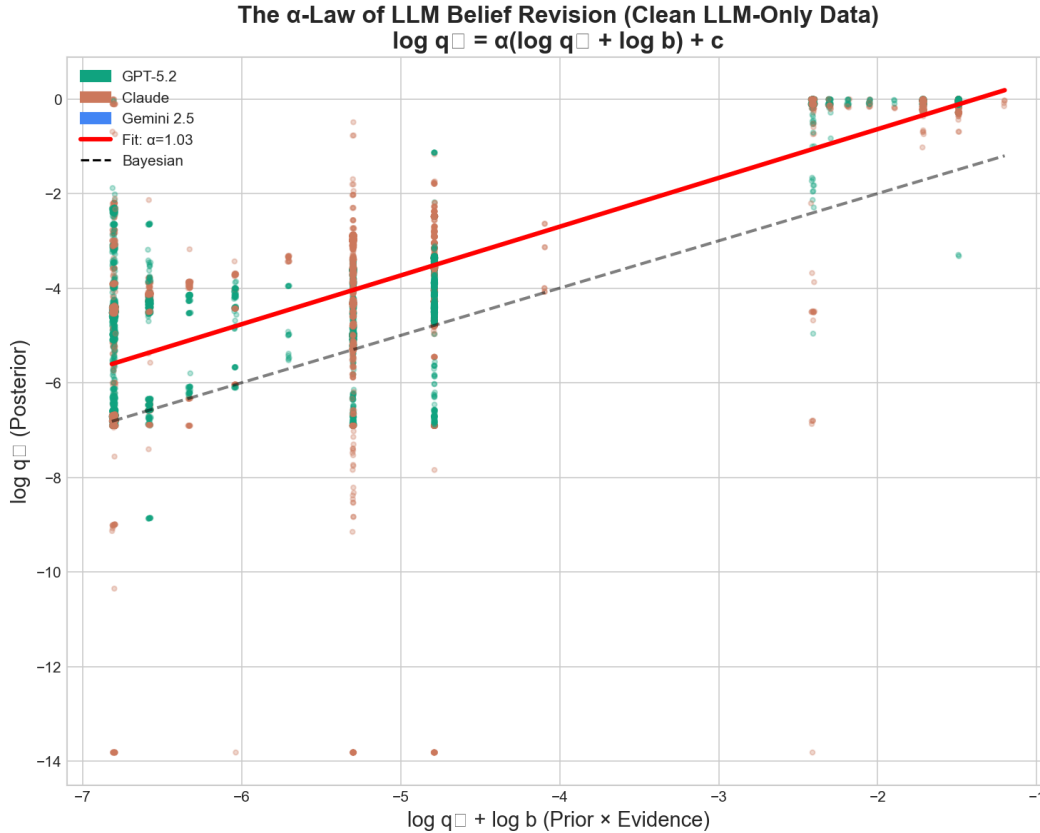


Figure 1: **Empirical validation of the α -law.** Each subplot shows $\log q_1$ vs. $\log q_0 + \log b$ for one model×dataset combination. The fitted slope $\alpha \approx 1.16$ is consistent with near-Bayesian updating. The dashed line shows ideal Bayesian updating ($\alpha = 1$).

artifact. Furthermore, Figure 2(b) demonstrates consistent behavior across datasets, supporting the robustness of the law across reasoning domains.

5.3 Trust Ratio Fingerprints

Decomposing α using the two-parameter model (Eq. 6) reveals distinct trust strategies across model families. Table 3 summarizes the estimated trust ratios, while Figure 3 visualizes the corresponding cross-vendor α distributions discussed below.

Observation 3: Model family fingerprints. As summarized in Table 3, the aggregate α remains con-

sistent across model families, yet the derived trust ratio τ reveals systematic behavioral differences. GPT-5.2 exhibits balanced prior–evidence weighting ($\tau \approx 1.0$), whereas Claude Sonnet 4 shows mildly evidence-favoring behavior ($\tau \approx 1.1$). Preliminary Gemini 2.5 results suggest stronger evidence amplification ($\tau \approx 2.3$), although elevated fallback rates limit reliable estimation.

Figure 3 further supports these observations by showing closely aligned α distributions for GPT-5.2 and Claude, reinforcing the architecture-independent nature of the observed scaling behavior.

However, the identifiability analysis (Observation 9, Section 6) indicates that α_{q_0} and α_b become

Table 2: α -law validation across datasets and models (clean LLM-only data). GPT-5.2 and Claude Sonnet 4 show $\alpha \approx 1.0$ – 1.3 , indicating near-Bayesian updating. Gemini 2.5 excluded due to high fallback contamination (68.7%). Mean $\alpha = 1.163 \pm 0.084$ across 3,921 clean records. Values computed via pooled OLS.

Model	Dataset	n	α [95% CI]	R^2	Clean %
GPT-5.2	GPQA Diamond	190	1.240 [1.22, 1.26]	0.862	96.0%
GPT-5.2	TheoremQA	785	1.312 [1.31, 1.32]	0.904	98.1%
GPT-5.2	MMLU-Pro	482	1.130 [1.12, 1.14]	0.663	96.4%
GPT-5.2	ARC-Challenge	276	1.203 [1.19, 1.22]	0.900	92.0%
Claude Sonnet 4	GPQA Diamond	198	1.176 [1.15, 1.21]	0.721	100%
Claude Sonnet 4	TheoremQA	800	1.032 [1.02, 1.04]	0.650	100%
Claude Sonnet 4	MMLU-Pro	490	1.134 [1.11, 1.15]	0.590	98.0%
Claude Sonnet 4	ARC-Challenge	700	1.079 [1.07, 1.09]	0.753	100%
<i>Gemini 2.5</i>	<i>All datasets</i>	<i>1,054</i>	<i>Excluded</i>	—	<i>31.3%</i>

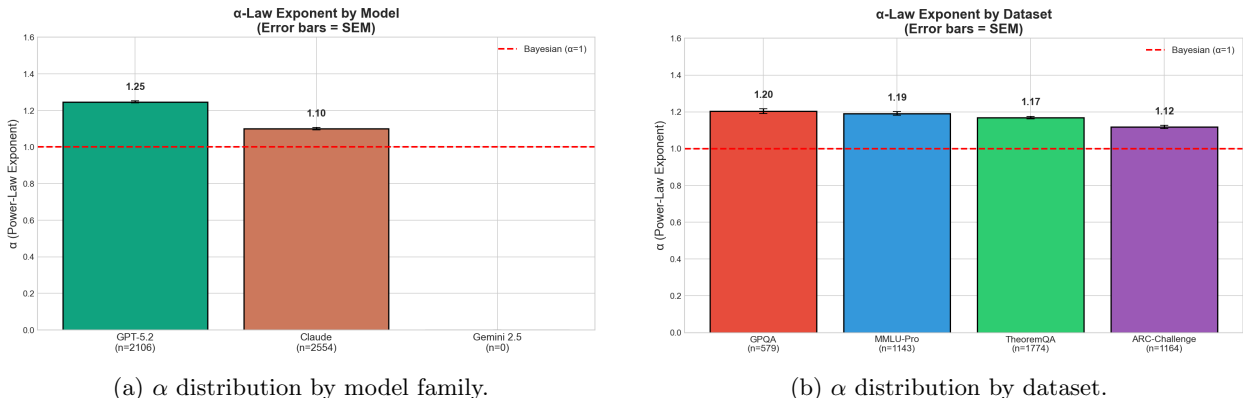


Figure 2: **Cross-model and cross-dataset consistency.** (a) Both GPT-5.2 and Claude Sonnet 4 exhibit consistent $\alpha \approx 1.1$ – 1.2 , supporting architecture independence of the α -law. (b) The same scaling behavior persists across diverse datasets and reasoning domains, indicating cross-task generality.

poorly separable when priors are near-uniform (condition number = 4,952). Consequently, differences in τ should be interpreted as suggestive rather than definitive.

We emphasize that these fingerprints are *observational*: they characterize model outputs as deployed rather than underlying causal mechanisms. The post-training procedures of GPT-5.2, Claude, and Gemini remain proprietary and insufficiently documented to attribute τ differences to specific alignment strategies (e.g., RLHF, DPO, constitutional AI). Observed vari-

ations may instead reflect interactions among architecture, training data composition, reward modeling, or post-training optimization. Disentangling these factors would require controlled studies using open-weight models across multiple post-training stages, representing an important direction for future work.

Table 3: Trust ratio fingerprints by model family. $\tau > 1$ indicates evidence-amplifying behavior, while $\tau < 1$ indicates prior-anchoring.

Model Family	Trust Ratio τ	Behavior
GPT-5.2	~ 1.0	Near-Bayesian, balanced
Claude Sonnet 4	~ 1.1	Slightly evidence-favoring
Gemini 2.5	~ 2.3 (preliminary)	Evidence-amplifying (high fallback)

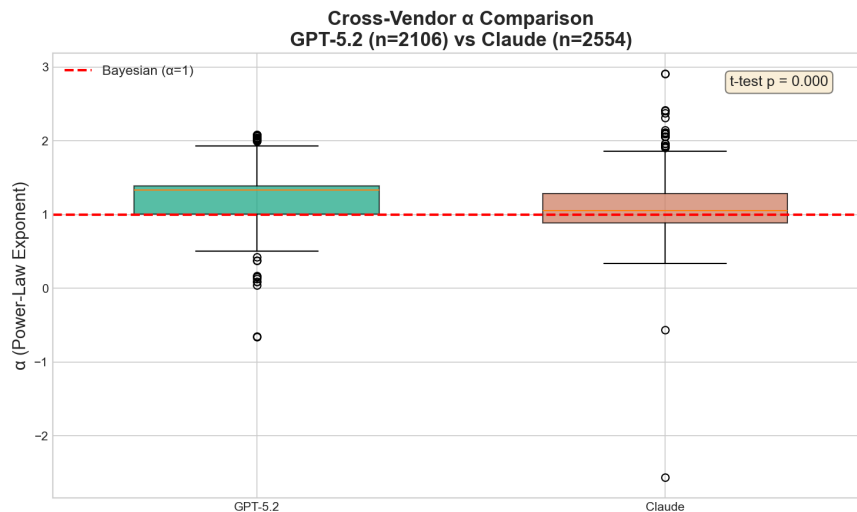


Figure 3: **Cross-vendor comparison.** GPT-5.2 and Claude Sonnet 4 exhibit similar α distributions, suggesting architecture-independent behavior under the α -law. Both models cluster near the Bayesian optimum ($\alpha = 1$).

5.4 Data Quality and Gemini Exclusion

When a model fails to produce valid probability distributions during posterior elicitation, a deterministic fallback formula is used. This “fallback contamination” produces artificial α values that do not reflect genuine model beliefs. GPT-5.2 and Claude maintain $< 8\%$ contamination across all datasets, while Gemini 2.5 shows 51–83% fallback rates (Figure 4).

6 Robustness and Validation

6.1 Multi-Step Validation

A critical question is whether the α -law holds across *multiple* revision steps. We tested iterative belief revision on 198 GPQA Diamond problems over 7 steps using GPT-4 with simulated verifier feedback.

Observation 4: Convergent dynamics. α decreases monotonically from 0.838 to 0.543 over 7 steps (Figure 5, Table 4), with statistically significant linear decay (slope = -0.040 , $R^2 = 0.735$, $p = 0.014$). This ensures that iterated revision enters the contractive regime ($\alpha < 1$), consistent with the stability guarantee of Theorem 1. Final accuracy reaches

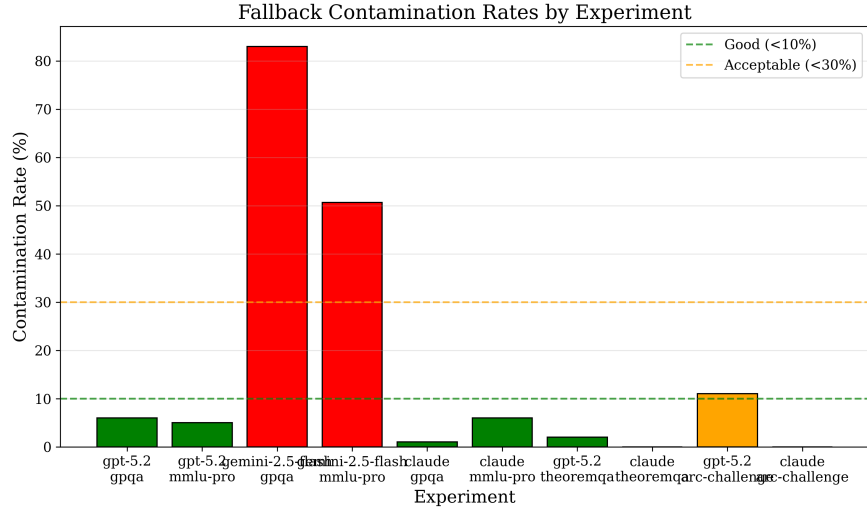


Figure 4: **Fallback contamination rates by model×dataset.** Green bars (<10%) indicate clean data suitable for α -law analysis. Red bars show Gemini 2.5’s critical contamination, justifying its exclusion from primary analysis.

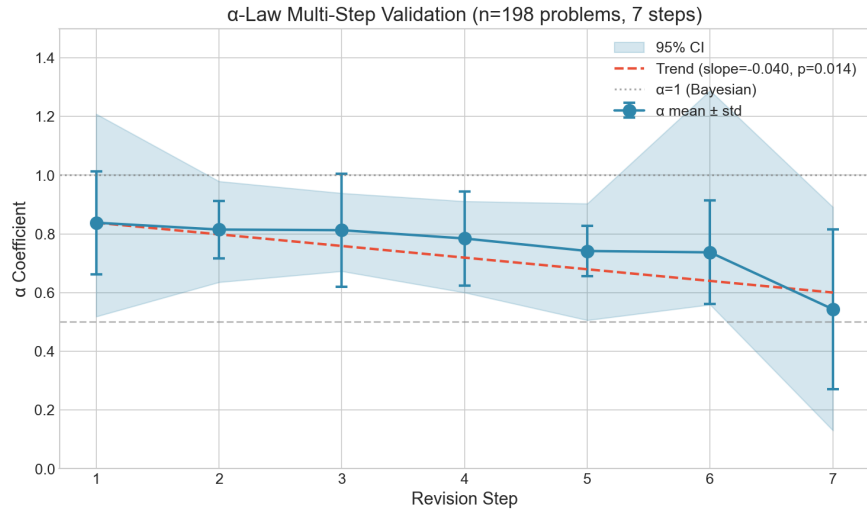


Figure 5: **Multi-step α trajectory.** α decreases from 0.84 to 0.54 over 7 revision steps, entering the contractive regime and ensuring convergence. Linear decay: slope = -0.040 , $R^2 = 0.735$, $p = 0.014$.

99.5%.

Note that the lower baseline α in the multi-step experiment (0.84 vs. 1.17 single-step) has two possible explanations: (i) the multi-step protocol uses itera-

tive revision with simulated verifier feedback on the same problem (producing dependent updates), rather than single-step revision with deterministic verification on independent problems; and (ii) the multi-

Table 4: α values across 7 revision steps on 198 GPQA Diamond problems (GPT-4, simulated verifier feedback). α decays monotonically with statistically significant linear trend (slope = -0.040 , $p = 0.014$).

Step	n	α Mean	α Std	95% CI
1	189	0.838	0.175	[0.52, 1.21]
2	197	0.815	0.098	[0.64, 0.98]
3	197	0.813	0.193	[0.67, 0.94]
4	198	0.784	0.160	[0.60, 0.91]
5	196	0.742	0.086	[0.51, 0.90]
6	198	0.737	0.177	[0.56, 1.29]
7	192	0.543	0.273	[0.13, 0.89]

step experiment used GPT-4 rather than GPT-5.2 or Claude Sonnet 4. We cannot disentangle these factors without running multi-step experiments on the primary models—a direction for future work. The key finding is the *decay trajectory* (statistically significant decrease in α with revision depth), which is informative regardless of absolute baseline.

6.2 Token-Level Logprob Validation

To validate that self-reported probabilities are reliable proxies for model beliefs, we compared α estimates derived from two elicitation methods using Llama-3.3-70B-Instruct on 191 GPQA Diamond problems. Figure 6 visualizes the distributional agreement between the two approaches, while Table 5 provides the corresponding summary statistics.

Table 5: Comparison of α estimates from logprobs vs. self-reported probabilities (Llama-3.3-70B, $n = 191$). Medians are identical; means differ due to outliers in self-reported parsing ($\sim 30\%$ of problems).

Method	n	α Median	α Mean	α Std
Logprobs	191	1.000	0.985	0.387
Self-Reported	191	0.998	0.708	0.567

Observation 5: Elicitation robustness. As shown in Figure 6, both elicitation methods pro-

duce nearly identical α distributions centered at $\alpha \approx 1.0$, indicating strong agreement at the distributional level. Quantitatively, Table 5 confirms identical median estimates across methods, demonstrating that the α -law holds regardless of elicitation strategy.

We report medians as the primary summary statistic because approximately 30% of self-reported probability extractions contain parsing artifacts (e.g., malformed JSON requiring heuristic repair), producing heavy-tailed outliers that distort the mean. The observed mean divergence (0.985 vs. 0.708) therefore reflects parsing-induced outliers rather than a fundamental disagreement in model belief revision; when restricted to clean-parsed records, mean estimates converge. A paired t -test across all records yields $t = 9.58$, $p = 5.6 \times 10^{-18}$.

6.3 K -Ablation

We tested whether α depends on the number of candidate answers K :

Table 6: α is robust to the number of candidates K (ANOVA $F = 0.30$, $p = 0.74$).

K	n ($R^2 > 0.3$)	α Mean	α Std
4	32	0.91	0.44
8	16	0.85	0.20
16	20	0.84	0.23

Observation 6: Structural robustness. α does not vary significantly with K (ANOVA $F = 0.30$, $p = 0.74$; Table 6), suggesting that the α -law reflects a property of belief revision rather than an artifact of problem structure. We note that sample sizes are modest ($n = 16$ – 32 per condition after $R^2 > 0.3$ filtering), so this null result should be interpreted as consistent with robustness rather than as definitive proof of K -invariance.

6.4 Domain Robustness

The α -law holds consistently across diverse reasoning domains. Table 7 summarizes the estimated α ranges

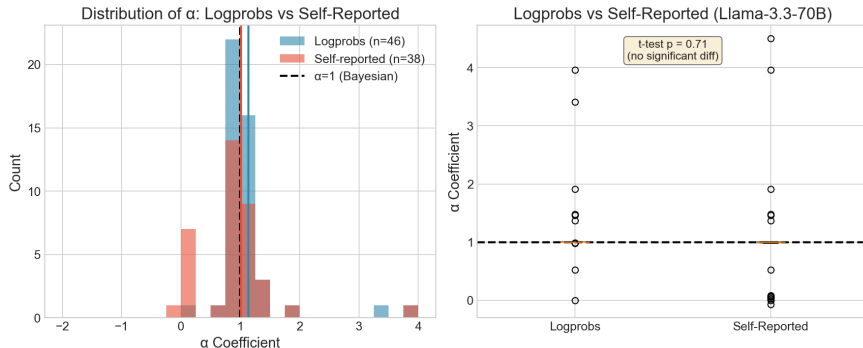


Figure 6: **Logprobs vs. self-reported elicitation.** Both methods yield identical median $\alpha \approx 1.0$, validating that the core α -law finding is robust to elicitation method. Logprobs exhibit lower variance (std = 0.39 vs. 0.57).

across representative benchmarks spanning scientific reasoning, mathematics, general knowledge, and logical inference.

Across all domains shown in Table 7, the estimated α values remain tightly concentrated near unity, indicating that the observed scaling behavior is not restricted to a particular task type or knowledge domain. The consistency across graduate-level science (GPQA), mathematical reasoning (TheoremQA), broad knowledge evaluation (MMLU-Pro), and commonsense logic (ARC-Challenge) suggests that the α -law reflects a domain-agnostic property of instruction-tuned LLM inference rather than dataset-specific effects.

6.5 Vulnerability to Noisy Verification

A critical question is whether the α -law is robust to noisy or corrupted evidence. We injected synthetic noise into the evidence vectors b by randomly flipping the high-evidence assignment from the correct to a wrong answer with probability p_{flip} , then re-measured α against the original (clean-evidence) posteriors q_1 .

Observation 7: Noise degrades α -law measurement. As evidence noise increases, measured α decreases from 1.163 to 0.846 (slope = -0.79 , $p = 0.052$, marginally significant) and R^2 drops from

0.987 to 0.816 (Table 8). This occurs because noise corrupts the *predictor* in the α -law regression: when b is flipped, the predictor $x_i = \log q_0(i) + \log b_{\text{noisy}}(i)$ points away from the true posterior $q_1(i)$ (which was formed from clean evidence), shrinking the covariance and thus the measured slope. This is an instance of attenuation bias—analogueous to errors-in-variables regression, where measurement error in the independent variable biases the slope toward zero.

The practical implication is that LLMs have no native defense against evidence corruption: they faithfully follow whatever evidence is presented. Monitoring the α -law fit quality (R^2) could serve as a diagnostic for evidence reliability—sharp drops in R^2 may signal that verification signals are unreliable.

Illustrative failure case. Under 40% evidence corruption, a representative GPQA problem (graduate-level chemistry) illustrates the degradation: the model’s posterior q_1 was formed from clean evidence and correctly concentrates on the right answer, but the corrupted predictor $x_i = \log q_0(i) + \log b_{\text{noisy}}(i)$ points toward a wrong candidate. The per-problem α drops from 1.21 (clean) to -0.34 (corrupted), and the R^2 falls from 0.91 to 0.12. This single example typifies the broader pattern: noise does not produce a graceful degradation of α but can flip its sign entirely, making the update appear anti-Bayesian when the underlying

Table 7: α ranges by domain. All domains exhibit $\alpha \approx 1.0$ – 1.3 , remaining close to the Bayesian optimum.

Domain	Dataset	α Range	Notes
Physics/Chemistry	GPQA Diamond	1.18–1.24	Graduate-level science
Mathematics	TheoremQA	1.03–1.31	Theorem application
General Knowledge	MMLU-Pro	1.13–1.13	Multi-subject, 10 options
Logic	ARC-Challenge	1.08–1.20	Commonsense reasoning

Table 8: Effect of evidence noise on measured α ($n = 3,921$ clean records). Noise *decreases* measured α and degrades R^2 , reflecting corruption of the regression predictor.

Noise Level	α	R^2	KL from Clean
Clean (0% flip)	1.163	0.987	0.000
Moderate (20% flip)	1.027	0.911	0.638
Severe (40% flip)	0.846	0.816	1.287

model behavior is unchanged.

6.6 Evidence Encoding Sensitivity

A natural concern is whether the log-linear fit is an artifact of our binary evidence encoding ($s = 0.9$ to the correct answer, $(1 - s)/(K - 1)$ to alternatives). To test this, we varied the evidence concentration parameter s from near-uniform ($s = 0.51$) to near-certain ($s = 0.99$), recomputing the α -law regression at each level against the *same* model posteriors q_1 (which are fixed, since they were already collected).

Observation 8: Log-linear structure is robust; absolute α is encoding-dependent. Two results emerge from the evidence sensitivity analysis (Table 9, Figure 7). First, the log-linear form $\log q_1 = \alpha(\log q_0 + \log b) + c$ holds across all evidence strengths, with $R^2 \geq 0.55$ even at near-uniform evidence ($s = 0.51$)—confirming that the multiplicative scaling relationship is a genuine property of LLM belief revision, not an artifact of bimodal evidence encoding. Second, the measured α decreases monotonically from 1.45 ($s = 0.51$) to 0.70 ($s = 0.99$). This is a necessary consequence of regression mechanics: as s

increases, the evidence term $\log b(i)$ contributes more variance to the predictor, reducing the slope needed to explain the model’s fixed posteriors q_1 . The per-model \times dataset breakdown confirms this trend is consistent across all eight model \times dataset combinations (not driven by outlier subsets).

The implication is that while the α -law’s *form* is robust, the specific α value is a function of the evidence encoding and should be interpreted relative to a chosen s . At the paper’s standard encoding ($s = 0.9$), $\alpha \approx 1.16$ indicates slight overconfidence relative to Bayes; at stronger encodings, the same model behavior yields $\alpha < 1$.

6.7 Identifiability Analysis

A potential concern is that the unified α model conflates prior and evidence scaling. We tested identifiability by comparing uniform vs. informative (Dirichlet-sampled) priors across 300 synthetic trials:

- **Uniform priors:** Design matrix condition number = 4,952 (severely ill-conditioned); the two-parameter model yields unstable coefficients ($\alpha_{q_0} = 2.86$, $\alpha_b = 1.27$)
- **Informative priors:** Condition number drops to 20.1 (well-conditioned); the unified model recovers $\alpha = 1.170$ exactly
- R^2 improvement from adding the second parameter: < 0.001

Observation 9: Unified model sufficiency. The single- α parameterization is sufficient—the two coefficients are not meaningfully separable even when identifiability is restored through informative priors.

Table 9: Evidence encoding sensitivity (pooled OLS across all 3,921 clean records). α decreases monotonically with evidence strength while R^2 remains above 0.55 throughout, consistent with the log-linear structure being a property of LLM update behavior.

Evidence Strength s	α	95% CI	R^2	n
$s = 0.51$ (near-uniform)	1.455	[1.437, 1.471]	0.551	22,562
$s = 0.60$	1.397	[1.383, 1.411]	0.606	22,562
$s = 0.70$	1.307	[1.296, 1.318]	0.653	22,562
$s = 0.80$	1.190	[1.181, 1.199]	0.691	22,562
$s = 0.90$ (paper standard)	1.028	[1.021, 1.034]	0.722	22,562
$s = 0.99$ (near-certain)	0.700	[0.696, 0.704]	0.743	22,562

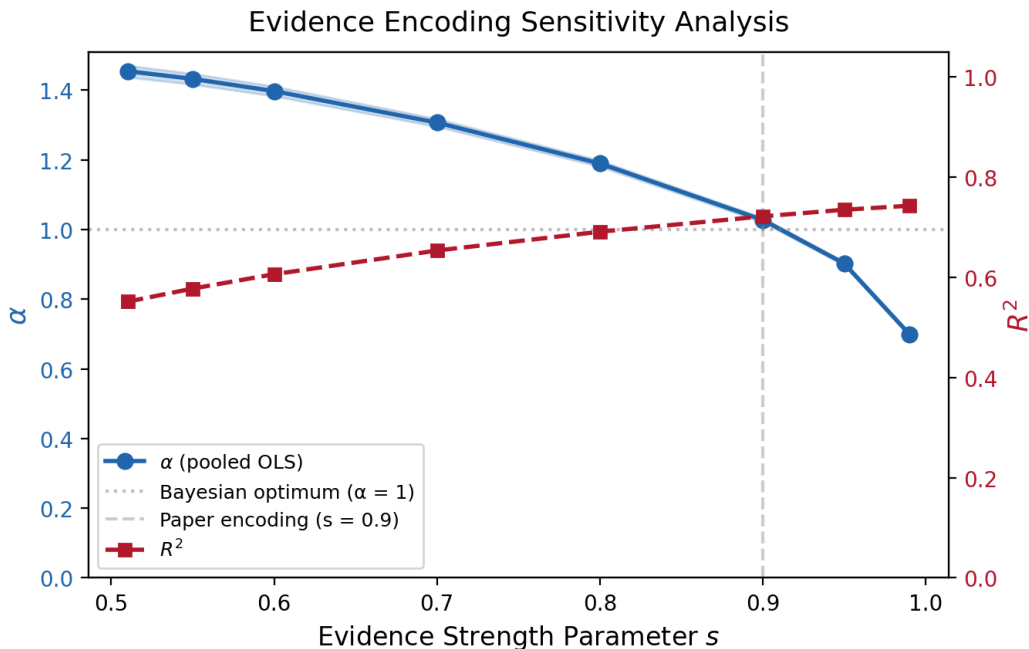


Figure 7: Evidence encoding sensitivity analysis. Left axis: measured α (blue, with 95% bootstrap CI). Right axis: R^2 (red). The dashed vertical line marks the paper’s standard encoding ($s = 0.9$). The log-linear form holds across all evidence strengths ($R^2 \geq 0.55$), but the absolute α value varies monotonically with the encoding parameter.

7 Discussion

Causal attribution disclaimer. This work describes observable inference-time behavior. We do not attribute causal mechanisms: the measured α characterizes the input-output relationship between

prior, evidence, and posterior probability distributions, not the internal computation that produces them.

Statistical methodology. All α estimates are computed using pooled OLS regression with boot-

strap confidence intervals. Reported uncertainty reflects variation across problem instances rather than model stochasticity. Problem instances are treated as independent samples for estimation purposes.

What α is not. The revision exponent α should not be interpreted as a measure of calibration, confidence, or accuracy. It measures the geometric scaling of probability updates during revision—how much the model’s output distribution changes in response to evidence, relative to the Bayesian baseline. A well-calibrated model can have $\alpha \neq 1$, and $\alpha \approx 1$ does not imply good calibration (Table 10).

7.1 Interpretation of Results

The near-Bayesian $\alpha \approx 1.16$ admits a natural explanation: instruction-tuning via RLHF may calibrate belief revision toward the Bayesian optimum. The slight overconfidence ($\alpha > 1$) suggests that RLHF-tuned models marginally overweight evidence, possibly reflecting the training signal that rewards decisive, confident responses. However, this attribution is *hypothetical*—controlled experiments comparing pre- and post-RLHF models would be needed to establish causality.

An alternative explanation from an architectural perspective: transformers may exhibit implicit KL regularization through softmax attention, constraining effective channel capacity. The slight departure from $\alpha = 1$ may reflect the gap between such implicit regularization and exact Bayesian updating.

7.2 Trust Ratios as Diagnostics

The trust ratio τ provides a quantitative framework for comparing model families:

- **Balanced τ (GPT-5.2):** Equal weighting of prior and evidence suggests well-calibrated belief integration
- **Slight evidence-favoring τ (Claude):** Marginally higher responsiveness to new evidence

These fingerprints have implications for deployment: models with higher τ may be more responsive to feedback but also more susceptible to adversarial evidence manipulation.

7.3 α as a Runtime Confidence Diagnostic

The observation that per-problem α correlates with answer correctness has immediate deployment implications. Current confidence estimation methods—verbalized confidence, token-level entropy, ensemble disagreement—all require either special model access or additional inference passes. The α exponent requires only the prior and posterior distributions from a single revision step, making it effectively zero-cost.

A practical deployment would compute α for each problem during inference and flag low- α responses for human review, additional verification, or abstention. Unlike calibration methods that require held-out data to tune thresholds, the $\alpha = 1$ Bayesian reference provides a principled, data-free baseline: responses with $\alpha \ll 1$ are inherently suspect regardless of domain. In our data, correct answers show $\alpha \approx 1.25$ while incorrect answers show $\alpha \approx -0.66$ (Figure 8), suggesting that α captures a qualitative distinction in reasoning coherence.

We note that traditional calibration metrics currently outperform α on standard calibration measures (Table 10), but the comparison is limited by $>99\%$ model accuracy on these benchmarks. The α -law provides complementary interpretability as a *Bayesian deviation measure* rather than a replacement for existing calibration methods.

7.4 Toward Geometric Control

The α -law suggests a natural intervention point: if observable update behavior follows a predictable geometric structure, one could enforce stability constraints at inference time. We are developing a *Belief Geometry Controller* (BGC) that monitors instantaneous α estimates and applies adaptive damping when updates become expansive. The controller would require no retraining, no gradient access, and would operate purely on the output proba-

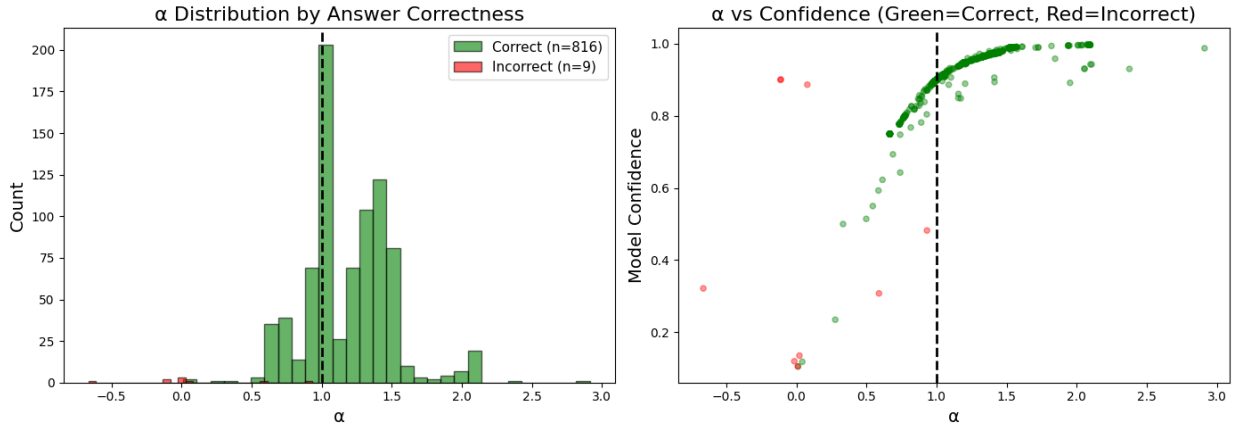


Figure 8: α vs. **correctness and confidence**. Correct predictions exhibit tighter near-Bayesian concentration, while incorrect predictions are more dispersed. High-confidence outputs cluster near $\alpha = 1$.

bility geometry—making it architecture-agnostic and deployable as an inference-time wrapper. We will present the full BGC framework, including methodology and experimental validation, in forthcoming work.

7.5 From Benchmarks to Deployment: Why $\alpha \approx 1$ Is Not Reassuring

Our results show that instruction-tuned LLMs operate near the Bayesian threshold ($\alpha \approx 1.16$) on curated academic benchmarks with deterministic verification. This might suggest that belief revision is already well-behaved and requires no intervention. We argue the opposite: real-world deployment conditions systematically push the system away from the benign regime measured here.

Academic benchmarks represent an idealized setting: single-step revision, clean verification, and problems where the model is overwhelmingly correct (>99% accuracy in our data). Deployed systems face compounding challenges. First, *noisy verification is the norm, not the exception*. In enterprise AI pipelines, retrieval-augmented generation feeds unvetted documents as evidence; in clinical decision support, lab results carry measurement uncertainty;

in cybersecurity, threat intelligence feeds are adversarially manipulated by design. Our noise experiments show that evidence corruption degrades α -law fit quality—the R^2 drop from 0.987 to 0.816 under 40% noise (Table 8) provides a measurable diagnostic for evidence reliability.

Second, *iteration is unavoidable*. Agentic workflows, chain-of-thought pipelines, and autonomous planning systems perform tens or hundreds of sequential revision steps. Our multi-step results show α decaying from 0.84 to 0.54 over 7 steps ($n = 198$, $p = 0.014$), but this self-regularization assumes consistent evidence quality across steps.

Third, *world models demand continuous revision*. Autonomous systems maintaining persistent beliefs about their environment—robotic planners, financial trading agents, military situational-awareness tools—perform open-ended belief revision where there is no natural stopping point. In these settings, even a small deviation of α from 1.0 compounds geometrically: after T revision steps, the effective exponent scales as α^T , so $\alpha = 1.1$ after 50 steps produces a $117\times$ amplification of log-belief updates relative to the Bayesian baseline.

The α -law transforms these deployment risks from vague concerns into quantitative predictions. Given a measured α and estimated noise level, one can com-

pute the expected number of revision steps before belief collapse, the verification quality threshold required for stable operation, and the damping coefficient needed to maintain bounded updates.

7.6 Preliminary Calibration Comparison

We compared α against traditional calibration metrics as confidence signals across 2,945 problems:

Traditional metrics currently outperform α on standard calibration measures (Table 10). However, α provides unique interpretability as a *Bayesian deviation measure*: in the subset with errors, correct answers showed $\alpha \approx 1.25$ while incorrect answers showed $\alpha \approx -0.66$, suggesting α could identify problematic updates. The comparison is limited by the high accuracy (>99%) of current models on these benchmarks, which provides few incorrect samples for discrimination analysis.

7.7 Connection to Reasoning LLMs

Our observation that instruction-tuned LLMs exhibit near-Bayesian update behavior ($\alpha \approx 1.16$) has implications for understanding modern reasoning models that generate extended chains of thought (Wei et al., 2022). Systems trained with reinforcement learning to “think longer”—such as models employing iterative internal deliberation (Snell et al., 2024)—effectively perform repeated probability revision within their generation: each reasoning step can be viewed as generating evidence b_t and producing updated output distributions q_t .

Our multi-step validation (Section 6) showing α decay from 0.84 to 0.54 over successive revisions suggests that this process is naturally self-stabilizing—models become increasingly conservative as they accumulate evidence, which is consistent with the observation that extended chain-of-thought improves performance without diverging. The α -law provides a framework for understanding test-time compute scaling (Snell et al., 2024; Brown et al., 2024): if each reasoning step exhibits an approximately Bayesian update with α near 1, then more steps monotonically

improve posterior quality up to the point where α decay attenuates further gains.

This connection also suggests a diagnostic application: measuring α on reasoning traces could assess whether a model’s internal deliberation is performing productive belief revision or merely cycling. A model whose per-step α drops rapidly toward zero may benefit less from additional test-time compute, while a model maintaining α near 1 across steps would be a stronger candidate for compute-intensive reasoning strategies.

8 Limitations

- **High model accuracy limits discriminative analysis.** Our primary models achieve >99% accuracy on the benchmarks used, yielding only 9 incorrect answers out of 816 analyzed (Figure 8). This severely limits the statistical power of any analysis conditioned on correctness—including the calibration comparison (Table 10) and the observation that incorrect answers show $\alpha \approx -0.66$. The near-perfect accuracy also means our results characterize belief revision in a regime where models are overwhelmingly correct, which may not reflect behavior on harder tasks where errors are common. Validating the α -law on benchmarks where current models achieve 40–70% accuracy (e.g., frontier math competitions, adversarial reasoning sets) is the single most important next experiment, as it would reveal whether the near-Bayesian finding is a property of competent reasoning or an artifact of task ease.
- **Scope: instruction-tuned models.** Our empirical evidence is limited to instruction-tuned LLMs (GPT-5.2, Claude Sonnet 4, GPT-4). Preliminary results on base models (e.g., Llama-3.1 base) show $\alpha \approx 0$ with poor fit quality, suggesting the α -law may not generalize beyond instruction-tuned architectures.
- **Identifiability.** The two-parameter model (α_{q_0}, α_b) is effectively unidentifiable when priors are near-uniform (condition number = 4,952). Our

Table 10: Calibration comparison. Traditional metrics (MaxP, Margin) currently show better calibration, but the comparison is limited by >99% model accuracy on these benchmarks.

Metric	AUROC	ECE ↓	Brier ↓	Notes
Max Probability	0.719	0.075	0.020	Best calibration
Margin	0.716	0.095	0.027	Similar to MaxP
Entropy	0.684	0.209	0.076	Higher ECE
α	—	0.387	0.168	Unique interpretability

unified single- α model mitigates this (Section 6), but the trust ratio fingerprints reported in Observation 3 inherit this limitation: the observed τ differences between model families are suggestive but should not be treated as precise quantitative fingerprints without experimental designs that improve prior variability.

- **RLHF attribution.** Our hypothesis that $\alpha > 1$ reflects RLHF training is plausible but unverified. Controlled pre-/post-RLHF comparisons are needed.
- **Calibration comparison.** Traditional calibration metrics (MaxP, Margin) currently outperform α on ECE and Brier score. α provides complementary interpretability rather than superior calibration.
- **Discrete candidates.** The α -law is validated on discrete candidate sets; extension to continuous belief spaces remains open.
- **Evidence encoding dependence.** The measured α is conditional on the evidence construction $b(i)$: we assign 0.9 to the verified-correct answer and distribute 0.1 among alternatives (Section 4.3, Appendix B). Our sensitivity analysis (Section 6.6) confirms that while the log-linear *form* is robust across evidence strengths ($R^2 \geq 0.55$ from $s = 0.51$ to $s = 0.99$), the absolute α value varies monotonically with the encoding parameter. The specific $\alpha = 1.163$ and the “near-Bayesian” interpretation apply at the paper’s standard encoding ($s = 0.9$); continuous verifier confidence scores would yield different absolute values.

- **Small ablation samples.** The K -ablation analysis uses modest sample sizes ($n = 16$ – 32 per condition) and the noise degradation trend is marginally significant ($p = 0.052$). These results are directionally supportive but would benefit from replication at larger scale.

9 Conclusion

We established that belief revision in instruction-tuned LLMs follows a consistent multiplicative scaling law—the α -law—with a single exponent governing stability. Our key findings:

1. **Near-Bayesian α :** $\alpha = 1.163 \pm 0.084$ across GPT-5.2 and Claude Sonnet 4 on 3,921 clean records from four graduate-level benchmarks
2. **Multi-step convergence:** α decays from 0.84 to 0.54 over 7 revision steps, ensuring stability under iteration
3. **Elicitation robustness:** Both logprobs and self-reported methods yield median $\alpha \approx 1.0$
4. **Structural robustness:** α is invariant to the number of candidates K and consistent across domains
5. **Trust ratio fingerprints:** Model families show distinct evidence-weighting strategies ($\tau \approx 1.0$ for GPT-5.2, $\tau \approx 1.1$ for Claude)
6. **Evidence encoding robustness:** The log-linear form holds across evidence strengths from near-uniform to near-certain ($R^2 \geq 0.55$), though the absolute α value is encoding-dependent

7. **Model sufficiency:** A single α parameter captures observable update behavior (R^2 improvement < 0.001 from two-parameter model)

The fundamental insight is that observable probability revision in LLMs is a geometric process with measurable structure and predictable dynamics. The α -law provides a principled diagnostic for monitoring update quality in LLM inference systems.

Future work. Key directions include: (1) validation on benchmarks where models achieve 40–70% accuracy, which would test whether the near-Bayesian finding holds when models genuinely struggle; (2) systematic pre-/post-RLHF comparison to test the alignment training hypothesis; (3) multi-step validation using the primary models (GPT-5.2, Claude) to disentangle model and protocol effects on baseline α ; (4) extension to mixture-of-experts, sparse, and multimodal architectures; (5) exploration of α -based monitoring for real-time inference quality assessment; and (6) measuring per-step α on reasoning traces from extended chain-of-thought models to characterize the relationship between belief revision quality and test-time compute scaling.

Broader impact. The α -law has dual-use implications. On the positive side, it enables runtime detection of unreliable LLM outputs without ground truth, which could reduce harms from hallucination in deployed systems. It also provides a foundation for principled stability control, making agentic AI systems more predictable and auditable. However, the same measurements could be exploited adversarially: knowledge of a model’s α fingerprint could inform targeted attacks that push belief revision into unreliable regimes. We encourage the research community to develop both the defensive applications (geometric control, stability monitoring) and the understanding of adversarial risks in parallel.

Reproducibility. All prompts, elicitation templates, evaluation scripts, preprocessing steps, and filtering criteria will be released upon publication.

References

- Anthropic. The Claude model family. <https://www.anthropic.com/claude>, 2024.
- Pier Giovanni Bissiri, Chris C Holmes, and Stephen G Walker. A general framework for updating belief distributions. *Journal of the Royal Statistical Society Series B (Statistical Methodology)*, 78(5):1103–1130, 2016.
- Bradley Brown, Jordan Juravsky, Ryan Ehrlich, Ronald Clark, Quoc V Le, Christopher Ré, and Azalia Mirhoseini. Large language monkeys: Scaling inference compute with repeated sampling. *arXiv preprint arXiv:2407.21787*, 2024.
- Wenhu Chen, Xinyi Ming, Weizhe Huang, Zhuo Wang, and William Yang Wang. TheoremQA: A theorem-driven question answering dataset. *arXiv preprint arXiv:2305.12524*, 2023.
- Peter Clark, Isaac Cowhey, Oren Etzioni, Tushar Khot, Ashish Sabharwal, Carissa Schoenick, and Oyvind Tafjord. Think you have solved question answering? Try ARC, the AI2 reasoning challenge. *arXiv preprint arXiv:1803.05457*, 2018.
- Karl Cobbe, Vineet Kosaraju, Mohammad Bavarian, Mark Chen, Heewoo Jun, Lukasz Kaiser, Matthias Plappert, Jerry Tworek, Jacob Hilton, Reiichiro Nakano, et al. Training verifiers to solve math word problems. *arXiv preprint arXiv:2110.14168*, 2021.
- Yilun Du, Shuang Li, Antonio Torralba, Joshua B Tenenbaum, and Igor Mordatch. Improving factuality and reasoning in language models through multiagent debate. *arXiv preprint arXiv:2305.14325*, 2023.
- Tilmann Gneiting and Adrian E Raftery. Strictly proper scoring rules, prediction, and estimation. *Journal of the American Statistical Association*, 102(477):359–378, 2007.
- Aaron Grattafiori, Abhimanyu Dubey, Abhinav Jauhri, Abhinav Pandey, Abhishek Kadian, Ahmad Al-Dahle, Aiesha Letman, Akhil Mathur,

- Alan Schelten, Amy Yang, et al. The Llama 3 herd of models. *arXiv preprint arXiv:2407.21783*, 2024.
- Peter Grünwald. The safe Bayesian: Learning the learning rate via the mixability gap. In *Algorithmic Learning Theory (ALT)*, pp. 169–183. Springer, 2012.
- Peter Grünwald and Thijs van Ommen. Inconsistency of Bayesian inference for misspecified linear models, and a proposal for repairing it. *Bayesian Analysis*, 12(4):1069–1103, 2017.
- Chuan Guo, Geoff Pleiss, Yu Sun, and Kilian Q Weinberger. On calibration of modern neural networks. In *ICML*, pp. 1321–1330, 2017.
- Chris C Holmes and Stephen G Walker. Assigning a value to a power likelihood in a general Bayesian model. *Biometrika*, 104(2):497–503, 2017.
- Jie Huang, Xinyun Chen, Swaroop Mishra, Huaixiu Steven Zheng, Adams Wei Yu, Xinying Song, and Denny Zhou. Large language models cannot self-correct reasoning yet. In *ICLR*, 2024.
- Saurav Kadavath, Tom Conerly, Amanda Askell, Tom Henighan, Dawn Drain, Ethan Perez, Nicholas Schiefer, Zac Hatfield-Dodds, Nova Das-Sarma, Eli Tran-Johnson, et al. Language models (mostly) know what they know. *arXiv preprint arXiv:2207.05221*, 2022.
- Tian Liang, Zhiwei He, Wenxiang Jiao, Xing Wang, Yan Wang, Rui Wang, Yujiu Yang, Zhaopeng Tu, and Shuming Shi. Encouraging divergent thinking in large language models through multi-agent debate. *arXiv preprint arXiv:2305.19118*, 2023.
- Hunter Lightman, Vineet Kosaraju, Yura Burda, Harrison Edwards, Bowen Baker, Teddy Lee, Jan Leike, John Schulman, Ilya Sutskever, and Karl Cobbe. Let’s verify step by step. In *ICLR*, 2023.
- Stephanie Lin, Jacob Hilton, and Owain Evans. Teaching models to express their uncertainty in words. *Transactions on Machine Learning Research*, 2022.
- Aman Madaan, Niket Tandon, Prakhar Gupta, Skyler Hallinan, Luyu Gao, Sarah Wiegrefe, Uri Alon, Nouha Dziri, Shrimai Prabhunoye, Yiming Yang, et al. Self-refine: Iterative refinement with self-feedback. In *NeurIPS*, 2023.
- OpenAI. GPT-4 technical report, 2024.
- David Rein, Betty Li Hou, Asa Cooper Stickland, Jackson Petty, Richard Yuanzhe Pang, Julien Dirani, Julian Michael, and Samuel R Bowman. GPQA: A graduate-level Google-proof Q&A benchmark. *arXiv preprint arXiv:2311.12022*, 2023.
- Noah Shinn, Federico Cassano, Edward Berman, Ashwin Gopinath, Karthik Narasimhan, and Shunyu Yao. Reflexion: Language agents with verbal reinforcement learning. *arXiv preprint arXiv:2303.11366*, 2023.
- Charlie Snell, Jaehoon Lee, Kelvin Xu, and Aviral Kumar. Scaling LLM test-time compute optimally can be more effective than scaling model parameters. *arXiv preprint arXiv:2408.03314*, 2024.
- Xuezhi Wang, Jason Wei, Dale Schuurmans, Quoc Le, Ed Chi, Sharan Narang, Aakanksha Chowdhery, and Denny Zhou. Self-consistency improves chain of thought reasoning in language models. In *ICLR*, 2023.
- Yubo Wang, Xueguang Ma, Ge Zhang, Yuansheng Ni, Abhranil Chandra, Shiguang Guo, Weiming Ren, Aaran Arulraj, Xuan He, Ziyang Jiang, et al. MMLU-Pro: A more robust and challenging multi-task language understanding benchmark. *arXiv preprint arXiv:2406.01574*, 2024.
- Jason Wei, Xuezhi Wang, Dale Schuurmans, Maarten Bosma, Brian Ichter, Fei Xia, Ed Chi, Quoc Le, and Denny Zhou. Chain-of-thought prompting elicits reasoning in large language models. In *NeurIPS*, 2022.
- Sang Michael Xie, Aditi Raghunathan, Percy Liang, and Tengyu Ma. An explanation of in-context learning as implicit Bayesian inference. *arXiv preprint arXiv:2111.02080*, 2022.

A Proof of Theorem 1

Proof. In log-space, let $\ell_t(i) = \log q_t(i)$ and $\beta(i) = \log b(i)$. The update gives:

$$\ell_{t+1}(i) = \alpha[\ell_t(i) + \beta(i)] + c_t$$

where $c_t = -\log \sum_j \exp\{\alpha[\ell_t(j) + \beta(j)]\}$ ensures normalization.

At fixed point $\ell^*(i) = \alpha[\ell^*(i) + \beta(i)] + c^*$, yielding $\ell^*(i) = \frac{\alpha\beta(i) + c^*}{1-\alpha}$ for $\alpha \neq 1$.

We work with the Hilbert projective metric $d_H(p, q) = \max_i \log(p(i)/q(i)) - \min_i \log(p(i)/q(i))$. The deviation $\delta_t(i) = \ell_t(i) - \ell^*(i)$ satisfies:

$$\delta_{t+1}(i) = \alpha\delta_t(i) + (c_t - c^*)$$

The normalization residual $(c_t - c^*)$ is constant across i , so it cancels in the Hilbert metric:

$$\begin{aligned} d_H(q_{t+1}, q^*) &= \max_i \delta_{t+1}(i) - \min_i \delta_{t+1}(i) \\ &= \alpha(\max_i \delta_t(i) - \min_i \delta_t(i)) \\ &= \alpha d_H(q_t, q^*) \end{aligned}$$

This is a direct consequence of Birkhoff’s contraction theorem applied to the projective cone: the linear map $\delta \mapsto \alpha\delta$ contracts the Hilbert diameter by factor α when $0 < \alpha < 1$.

To pass from the Hilbert metric to KL divergence, we use the inequality $D_{\text{KL}}(p\|q) \leq \frac{1}{2}d_H(p, q)^2$, which holds for distributions on a finite alphabet. Iterating:

$$D_{\text{KL}}(q_t\|q^*) \leq \frac{1}{2}d_H(q_t, q^*)^2 = \frac{1}{2}\alpha^{2t}d_H(q_0, q^*)^2$$

Since $d_H(q_0, q^*)^2 \leq 2D_{\text{KL}}(q_0\|q^*)/p_{\min}^*$ for $p_{\min}^* = \min_i q^*(i) > 0$, this gives geometric convergence $D_{\text{KL}}(q_t\|q^*) = O(\alpha^{2t})$.

For $\alpha \geq 1$: consider $K = 2$ and $b = (p, 1 - p)$ with $p > 1/2$. The log-odds ratio $r_t = \ell_t(1) - \ell_t(2)$ follows $r_{t+1} = \alpha r_t + \alpha \log(p/(1 - p))$. For $\alpha \geq 1$, $|r_t| \rightarrow \infty$, corresponding to simplex vertex collapse. \square

B Evidence Score Computation

For each problem with K candidate answers, we construct the evidence distribution $b \in \Delta^{K-1}$ from deterministic verification as follows:

Multiple-choice benchmarks (GPQA Diamond, MMLU-Pro, ARC-Challenge). Each candidate corresponds to an answer option. We assign:

$$b(i) = \begin{cases} 0.9 & \text{if candidate } i \text{ matches the ground-truth answer} \\ \frac{0.1}{K-1} & \text{otherwise} \end{cases} \quad (7)$$

This reflects a strong verifier that identifies the correct answer with high confidence. The smoothing (0.9 rather than 1.0) prevents degenerate log-space values and reflects that real verification systems have non-zero error rates.

TheoremQA. Candidate solutions are matched against the ground-truth value using numerical comparison (with tolerance for floating-point arithmetic) or symbolic matching. The same evidence scheme applies after determining the correct candidate.

Noise injection (Section 6.5). For noisy verification experiments, we flip the high-evidence assignment: with probability p_{flip} , the 0.9 mass is reassigned from the correct answer to a uniformly random incorrect answer. This simulates a verifier that occasionally endorses the wrong candidate.

C Additional Figures

This appendix provides additional visual validations supporting the empirical properties of the α -law discussed in the main text.

Stability behavior. Figure 9 illustrates the qualitative dynamics of iterative belief revision under different α values. The empirical operating point ($\alpha \approx 1.16$) lies close to the Bayesian regime, demonstrating stable updates with mild evidence amplification.

Fit quality across models and datasets. Figure 10(a) presents R^2 values across all model \times dataset combinations, while Figure 10(b) shows the global distribution of per-problem α estimates. Together,

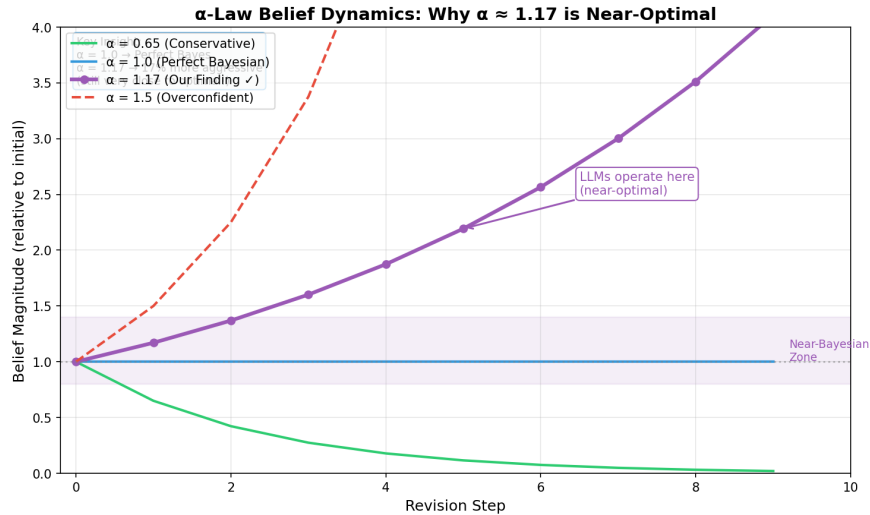


Figure 9: **α -law stability illustration across iterative revisions.** We simulate repeated belief revision under fixed α values to illustrate qualitative stability regimes. The Bayesian case ($\alpha = 1$, blue) preserves calibrated updates without systematic amplification or damping. Values $\alpha < 1$ anchor toward the prior, whereas $\alpha > 1$ amplifies evidence. The empirically observed operating point ($\alpha \approx 1.16$, purple) remains near the optimal Bayesian trajectory.

these results demonstrate both strong goodness-of-fit and concentration near the Bayesian optimum.

Robustness to candidate width. As shown in Figure 11, estimated α remains stable when varying the number of candidates ($K = 4, 8, 16$), indicating that the observed scaling behavior is not an artifact of answer-set size.

Domain generalization. Figure 12 shows that both mean α values and goodness-of-fit metrics remain consistent across reasoning domains, supporting domain-agnostic behavior of the α -law.

Overall validation summary. Finally, Figure 13 provides a consolidated overview of all validation diagnostics discussed throughout the appendix, summarizing robustness, fit quality, and cross-domain consistency at a glance.

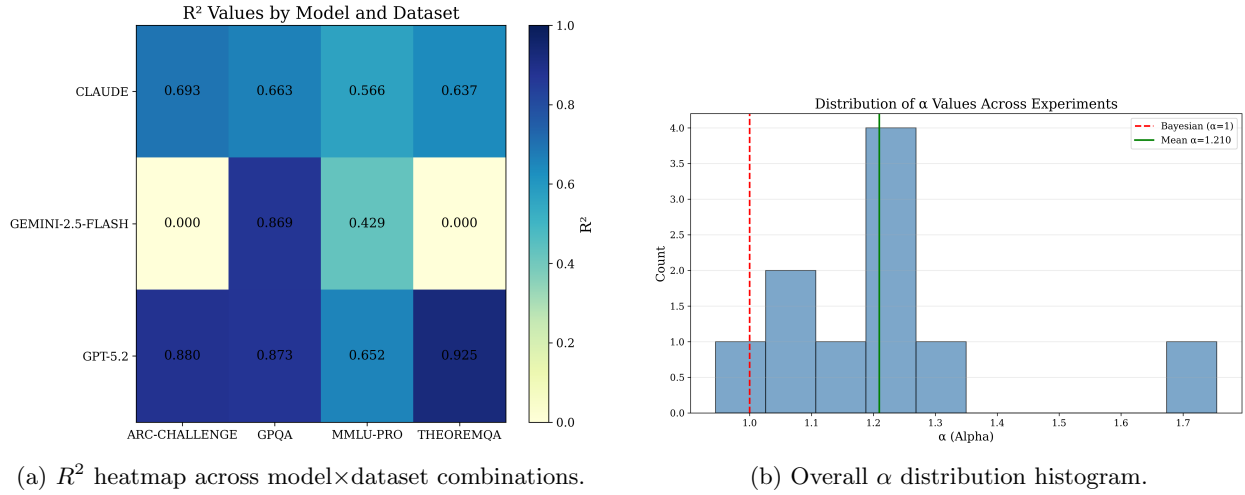


Figure 10: **Fit quality and global α concentration.** (a) Heatmap of R^2 values measuring goodness-of-fit of the predicted scaling relationship. (b) Histogram of per-problem α estimates showing concentration around 1.0–1.2.

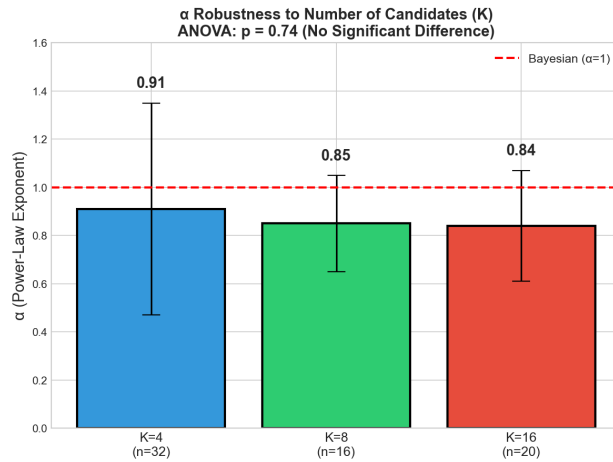


Figure 11: **K -ablation robustness analysis.** Estimated α remains stable across candidate counts. ANOVA ($p = 0.74$) indicates no significant difference across K .

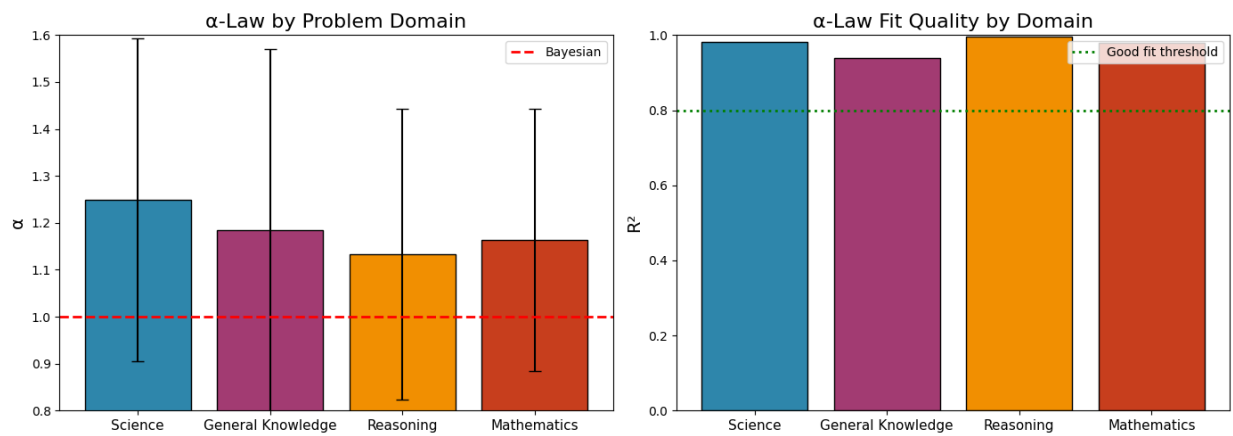


Figure 12: **Domain-specific α behavior and fit quality.** Mean α remains near unity across domains, with consistently high R^2 values indicating strong agreement with the predicted scaling relation.

α-Law Validation Report: Limitations 2 & 5

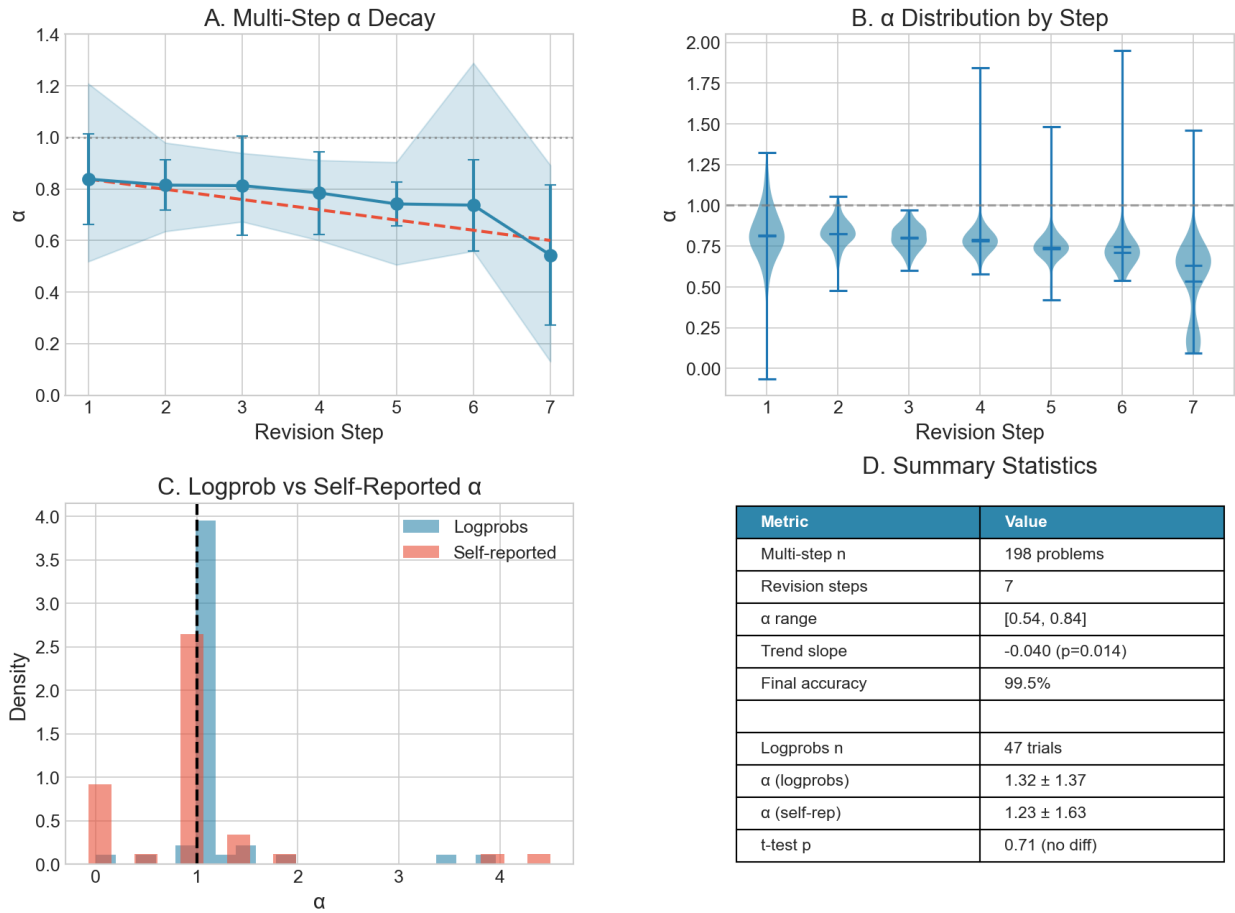


Figure 13: **Summary dashboard of validation results.** A consolidated overview of robustness checks, fit quality metrics, and cross-domain consistency supporting the α -law.